

Argon treatment after experimental subarachnoid hemorrhage: evaluation of microglial activation and neuronal survival as a subanalysis of a randomized controlled animal trial

Benedikt Kremer¹, Mark Coburn², Agnieszka Weinandy¹, Kay Nolte³, Hans Clusmann¹, Michael Veldeman¹, Anke Höllig^{1,*}

¹ Department of Neurosurgery, RWTH Aachen University Hospital, Aachen, Germany

² Department of Anaesthesiology, RWTH Aachen University Hospital, Aachen, Germany

³ Institute of Neuropathology, RWTH Aachen University Hospital, Aachen, Germany

*Correspondence to: Anke Höllig, MD, ahoellig@ukaachen.de.

orcid: 0000-0001-6798-5703 (Anke Höllig)

Abstract

Hereinafter, we evaluate argon's neuroprotective and immunomodulatory properties after experimental subarachnoid hemorrhage (SAH) examining various localizations (hippocampal and cortical regions) with respect to neuronal damage and microglial activation 6, 24 and 72 hours after SAH. One hour after SAH (endovascular perforation rat model) or sham surgery, a mixture of gas containing 50% argon (argon group) or 50% nitrogen (control group) was applied for 1 hour. At 6 hours after SAH, argon reduced neuronal damage in the hippocampal regions in the argon group compared to the control group ($P < 0.034$). Hippocampal microglial activation did not differ between the treatment groups over time. The basal cortical regions did not show a different lesion pattern, but microglial activation was significantly reduced in the argon group 72 hours after SAH ($P = 0.034$ vs. control group). Whereas callosal microglial activation was significantly reduced at 24 hours in the argon-treated group ($P = 0.018$). Argon treatment ameliorated only early hippocampal neuronal damage after SAH. Inhibition of microglial activation was seen in some areas later on. Thus, argon may influence the microglial inflammatory response and neuronal survival after SAH; however, due to low sample sizes the interpretation of our results is limited. The study protocol was approved by the Government Agency for Animal Use and Protection (Protocol number: TVA 10416G1; initially approved by the "Landesamt für Natur, Umwelt und Verbraucherschutz NRW," Recklinghausen, Germany, on April 28, 2009).

Key words: argon; early brain injury; experimental subarachnoid hemorrhage; Iba-1; microglial activation; neuroinflammation; neuronal survival; neuroprotection

doi: 10.4103/2045-9912.296039

How to cite this article: Kremer B, Coburn M, Weinandy A, Nolte K, Clusmann H, Veldeman M, Höllig A. Argon treatment after experimental subarachnoid hemorrhage: evaluation of microglial activation and neuronal survival as a subanalysis of a randomized controlled animal trial. *Med Gas Res.* 2020;10(3):103-109.

Funding: This study was supported by the Start Program, RWTH Aachen, Germany.

INTRODUCTION

Subarachnoid hemorrhage (SAH) is a less common subtype of stroke accounting for about five percent of all of the stroke cases.¹ Patients suffering from SAH are usually younger than those affected by ischemic stroke.² Nevertheless, the case fatality after SAH is around 50% and the mortality rates of the survivors are enormous (indicated by standardized mortality ratios of 1.7 (95% confidence interval 1.4–2.1) overall and 3.2 (95% confidence interval 0.8–13.1) for patients < 40 years).³

Spontaneous SAH is usually caused by the rupture of a cerebral aneurysm.⁴ The rupture of an intracranial aneurysm causes a sudden impact with arterial pressure into the subarachnoid space. This results in a sudden increase of the intracranial pressure (ICP), in a short-term global ischemia and in a destruction of the blood-brain barrier.

The damaging mechanisms in the first 72 hours after the event of bleeding are summarized under the term early brain injury.⁵ The extent of damage within this timeframe also determines the likelihood of secondary damage such as delayed cerebral ischemia, which is a major cause of secondary mortality and morbidity and still comprises an entity difficult to treat.⁶ So far, no specific therapeutic options for the treatment

of early brain injury have been established in clinical practice.

Argon is an inert noble gas that is not chemically reactive, and thus it easily overcomes the blood-brain barrier. However, it shows biological effects, in particular neuroprotective effects, which could be detected in previous studies. The exact mechanism behind these effects and their temporal dynamics is not yet clear.^{7,8}

Using *in vitro* experiments with organotypic hippocampus sections, these neuroprotective effects could be demonstrated both in a model of traumatic brain injury and in an ischemic model with oxygen and glucose deprivation.⁹

In vivo, this neuroprotective effect also has been confirmed in the middle cerebral artery occlusion ischemia model^{10,11} and, later on, also for the SAH model showing a decreased neuronal damage in the hippocampal region for the argon-treated animals.¹² Both neuroprotective effects as well as the reduction of the secondary inflammation in terms of microglial activation have also been demonstrated for xenon treatment after experimental SAH.¹³ However, argon has distinct advantages over xenon applied as a therapeutic. It does not show any narcotic effects and it is financially more cost-effective, which makes subsequent use much more realistic.

We therefore aim to analyze the neuroprotective effect of argon after experimental SAH depending on time after SAH as well as localization examining various cortical and hippocampal regions of interest in order to depict more detailed and accurate patterns of the effects after treatment with argon. Further, the influence of argon on the delayed activation of microglia determining to a major extent secondary injury will be examined.

MATERIALS AND METHODS

Study design

This is a subanalysis of a randomized controlled animal trial examining the neuroprotective effects of argon inhalation (50% for 1 hour) with treatment initiation 1 hour after SAH induction. Three observation times were applied resulting in a total of 12 groups. The primary outcome was neuronal damage on the left hemisphere. The secondary outcome was microglial activation.

Ethical statement

All of the experiments were conducted in accordance with the Guide for Care and Use of Laboratory Animals (National Research Council, and the Committee for the Update of the Guide for the Care and Use of laboratory Animals; 8th edition 2011). The study protocol was approved by the Government Agency for Animal Use and Protection (Protocol number: TVA 10416G1; initially approved by the “Landesamt für Natur, Umwelt und Verbraucherschutz NRW,” Recklinghausen, Germany, on April 28, 2009). “The Animal Research: Reporting of *In Vivo* Experiments guidelines”¹⁴ were used as criteria for adequate performance and reporting of experiments.

Animals

Sprague-Dawley rats (male, age around 9 weeks, body weight 300–400 g, Charles River, Sulzfeld, Germany) were used for the experiments. They were kept in a specific pathogen-free shelter under a 12-hour light/dark cycle for at least 1 week prior to the start of the experiments. Appropriate food was provided. Before starting the experiments, the animals were first randomized by drawing a lot to a sham or a SAH group and second to a treatment and a control group. The experimental groups were defined as follows: sham nitrogen (N₂) (ventilation with 50% O₂/50% N₂ 1 hour after sham surgery for 1 hour), sham Ar (ventilation with 50% O₂/50% Ar (argon) 1 hour after sham surgery for 1 hour), SAH N₂ (ventilation with 50% O₂/50% N₂ 1 hour after SAH induction for 1 hour) and SAH Ar (ventilation with 50% O₂/50% Ar 1 hour after SAH induction for 1 hour).

Experimental procedure

To induce SAH we used the modified endovascular perforation model.^{15,16} During the entire procedure ICP and cerebral blood flow were monitored. To initiate anesthesia, the animals received midazolam (2 mg/kg), medetomidine (0.15 mg/kg) and fentanyl (0.0075 mg/kg) via intraperitoneal injections.¹⁷ Anesthesia was maintained by further regular injections of a quarter of the induction dose in 30–45-minute intervals. Postoperatively, analgesia with metamizole (20 mg/kg) was

continued via intramuscular injections until euthanasia (6, 24 or 72 hours after SAH induction). To maintain the physiological body temperature of 37°C, a heating pad (Physitemp Instruments, Inc., Clifton, NJ, USA) was used. One left and one right laser Doppler flowmetry probes were placed in proximity of the bregma to measure regional cerebral blood flow (Moor Instruments, Axminster, Devon, UK). Parietal on the left side, an ICP probe was implanted in order to measure the ICP continuously (Microsensor/Codman ICP Express Monitor, Codman/De Puy, Raynham, MA, USA). SAH was induced by the modified endovascular perforation model initially described by Park et al.¹⁶ First, the common carotid artery on the left side was dissected and the internal carotid artery was identified. Subarachnoid hemorrhage was then induced by vascular perforation with a wolfram wire after intravascular advancement of a tube (containing the wire) into the internal carotid artery on the left side. A successful induction of subarachnoid hemorrhage was demonstrated by a sudden increase in ICP and a bilateral decrease in regional cerebral blood flow. For the sham operated animals, the exact same procedure was carried out except for vascular perforation.

One hour after SAH induction or sham surgery, the ventilation was switched to either a mixture of 50% O₂/50% argon (Air Liquide, Paris, France) or 50% O₂/50% N₂ (control group) for 1 hour. Euthanasia was performed 6, 24 or 72 hours after SAH induction by decapitation after exsanguination under deep anesthesia. The brains of the animals were then removed and cut into 2 mm coronal slices. These slices were then fixated in paraformaldehyde and embedded in paraffin.

Histology/immunohistochemistry

Paraffin embedded brain slices were cut in 2 μm thick sections. Two slices were selected from the area 3.6 mm caudal of the bregma. After placing the sections on silane-coated slides they were deparaffined. One section per animal was hematoxylin-eosin stained. The other section was incubated with anti-ionized calcium-binding adapter molecule 1 (Iba-1; 1:500; Wako Chemicals, Neuss, Germany) as primary antibody diluted in blocking solution after rehydration, blocking of the endogenous peroxidase activity and heating in citrate buffer for antigen retrieval and after blocking of non-specific binding by incubation in phosphate buffer saline containing 2% normal goat serum. Finally, an appropriate biotinylated secondary rabbit antibody was used (1:200; Vector Laboratories Ltd., Peterborough, UK) for visualization via a DAB Peroxidase Substrate Kit (Vector Laboratories Ltd.).

Neuronal cell damage

Hematoxylin-eosin sections were made to assess neuronal damage. Seven regions of interest (ROIs) were defined (five hippocampal regions: cornu ammonis (CA)1, CA2, CA2/3, CA3, and dentate gyrus and two cortical regions: postero-lateral cortex (PLCo) and postero-medial cortex (PMCo); selected according to Paxinos and Watson¹⁸). These regions were counted in a standardized fashion using a 400-fold magnification. In the ROIs defined areas were photographed with an AxioScope A1 microscope with an AxioCam MRc (ZEISS, Jena, Germany) and the ZEN lite

2011 software (ZEISS) for three times. Neuronal death was assessed according to anatomical hallmarks such as nuclear condensation (pyknosis), hypereosinophilic and shrunken cytoplasm. Vital and dead neurons in the photographed areas were distinguished, marked and counted using Adobe Photoshop CS2 (Adobe Systems Software Ireland Limited, Dublin, Republic of Ireland). A ratio of dead neurons/total neurons was formed for each ROI examined. Furthermore, the mean values of the single ROIs were summarized in the anatomically defined areas. Sum scores were thus created for the hippocampus and the basal cortex. To calculate the sum scores, the mean values of the single ROIs were summed up and averaged again.

Microglial activation

For the evaluation of the microglial activation, sections were stained with the antibody against Iba-1. Here, the microglial activation was quantified in eight regions of interest (five in the hippocampal regions: CA1, CA2, CA2/3, CA3, and dentate gyrus, two cortical regions: PLCo and PMCo and the corpus callosum as a representative of the white matter).

For the quantification, an absolute cell count of activated microglia in a high-power field (400-fold magnification) was performed. The five hippocampal, the two cortical regions of interest and the corpus callosum as a ROI were photographed three times per animal. The absolute number of activated Iba-1-positive cells was counted out in the CA1, CA2, CA2/3, CA3, dentate gyrus, PLCo, and PMCo of the left hemisphere and also in the corpus callosum. Additionally, sum scores were created for the hippocampus and the basal cortex.

Statistical analysis

Sample size calculation was extrapolated from previous studies^{12,13} resulting in an estimated sample size of $n = 7$ per treatment group (effect size estimation according to the results of neuronal damage after SAH after xenon treatment). Sample size was estimated according to the previously depicted calculation (G*Power 3.9.1.2 downloaded at <http://www.gpower.hhu.de/>).¹³ All statistical analyses were performed using SPSS v 25.0 (IBM SPSS Inc., Chicago, IL, USA). All graphics were acquired using GraphPad Prism (GraphPad Software Inc., La Jolla, CA, USA).

For statistical analysis of neuronal cell death and microglial activation repeated measures analysis of variance was applied analyzing the superordinate regions (hippocampus, basal cortex and corpus callosum). For statistical analysis of the ICP an unpaired t -test was used. All data are presented as mean \pm SD unless stated otherwise. A P -value of < 0.05 was considered statistically significant.

RESULTS

Baseline analysis of experimental animals

A total of 83 animals have been analyzed. One animal had to be excluded due to premature death (not fulfilling the initially planned observation period), six animals in the sham group had to be excluded due to tissue damage caused by cerebral blood flow probes, and ten animals had to be excluded as the hippocampal region was not properly depicted in the available brain slices. Finally, 66 animals were included (**Figure 1**).

During the induction of SAH the peak ICP was documented. With regards to the experimental groups 6 and 24 hours after SAH, ICP did not differ significantly between the treatment groups, whereas the argon treatment group (observation time: 72 hours after SAH) showed a significantly higher ICP than the control group (6 hours after SAH: $P = 0.289$; 24 hours after SAH: $P = 0.791$; 72 hours after SAH: $P = 0.014$; unpaired t -test; **Figure 2**). No adverse events due to argon administration were detected.

Effect of argon on neuronal cell damage in the brain of SAH rats

Neuronal cell death was assessed using hematoxylin and eosin stained section based on anatomical hallmarks such as nuclear condensation (pyknosis), hypereosinophilic and shrunken cytoplasm. Hippocampal and cortical ROIs were defined according to the anatomical landmarks (**Figure 3**) and apoptotic neurons per total neurons (within a single ROI) were counted indicating neuronal damage.

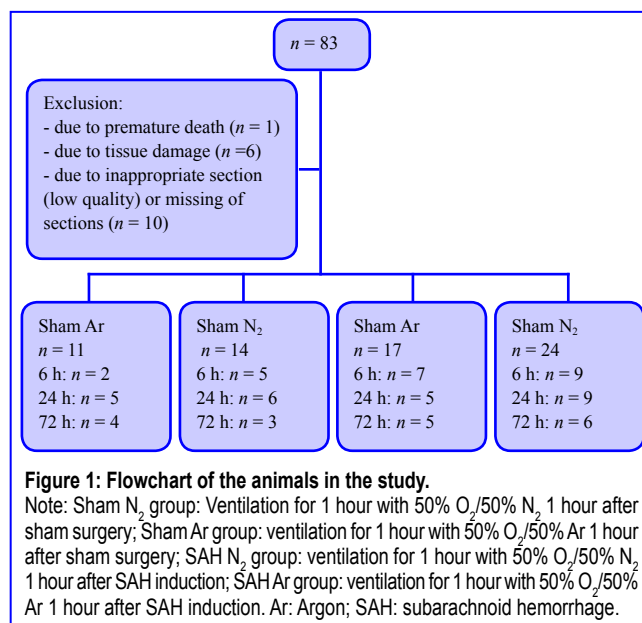


Figure 1: Flowchart of the animals in the study.

Note: Sham N₂ group: Ventilation for 1 hour with 50% O₂/50% N₂ 1 hour after sham surgery; Sham Ar group: ventilation for 1 hour with 50% O₂/50% Ar 1 hour after sham surgery; SAH N₂ group: ventilation for 1 hour with 50% O₂/50% N₂ 1 hour after SAH induction; SAH Ar group: ventilation for 1 hour with 50% O₂/50% Ar 1 hour after SAH induction. Ar: Argon; SAH: subarachnoid hemorrhage.

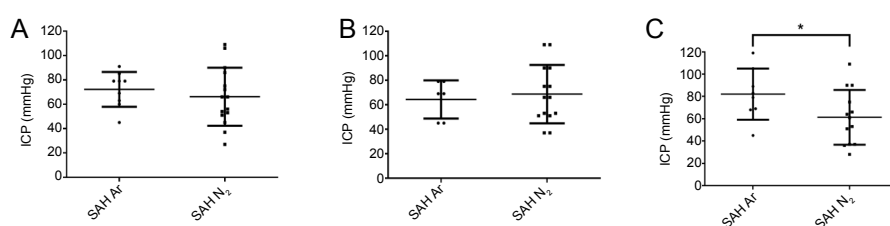


Figure 2: Peak ICP of the SAH rats with argon or N₂ treatment at 6 (A), 24 (B) and 72 hours (C).

Note: Data are expressed as mean \pm SD. * $P < 0.05$ (unpaired t -test). SAH N₂ group: Ventilation for 1 hour with 50% O₂/50% N₂ 1 hour after SAH induction; SAH Ar group: ventilation for 1 hour with 50% O₂/50% Ar 1 hour after SAH induction. Ar: Argon; ICP: intracranial pressure; SAH: subarachnoid hemorrhage.

The detailed analyses are shown in **Table 1**.

Summing up the results for the specific regions 6 hours after SAH a significantly less damage in the hippocampus was seen in the argon-treated group (6 hours after SAH: $P = 0.034$; repeated-measures analysis of variance), which 24 hours and 72 hours after SAH was no more detectable ($P = 0.324$; $P = 0.436$; repeated-measures analysis of variance) (**Figure 4**). With regard to the cortical ROIs the sum score (PMCO + PLCO) no significant difference was seen over time (6 hours after SAH: $P = 0.434$; 24 hours after SAH: $P = 0.305$; 72 hours after SAH: $P = 0.539$; repeated measures analysis of variance) (**Figure 5**).

Microglial activation in the brain of the SAH rats with argon or N₂ treatment

Iba-1 is a protein expressed in the cytoplasm, which is highly specific for microglia. Activation of microglia is associated with an increase of Iba-1 expression.^{19,20} Therefore, Iba-1 expression has been used as a surrogate marker for microglia activation. We analyzed the Iba-1 positive cells presenting a microglial habitus in eight ROIs (five hippocampal regions, two cortical regions and the corpus callosum) in order to identify the effect of argon treatment on secondary inflammatory reaction after SAH. Iba-1-positive cells were quantified in the CA1, CA2, CA2/3, CA3, dentate gyrus, PLCo, and PMCo of the left hemisphere and also in the corpus callosum. The detailed analyses are shown in **Table 2**.

In the early phase after SAH (6 hours) no significant difference with regard to microglia activation was seen most probably due to the time-dependent activation of microglia with a peak around 2 days after injury. Detailed results for

Table 1: Neuronal damage in percent (%) in the hippocampal CA1, CA2, CA2/3 and DG, and cortical PLCo and PMCo regions of SAH rats

	SAH Ar	SAH N ₂	P-value
6 h after SAH			
CA1	17.51±22.87	40.08±32.48	0.142
CA2	23.45±22.86	53.11±26.45	0.034
CA2/3	33.96±21.96	57.64±22.91	0.056
CA3	36.73±16.28	60.09±21.63	0.032
DG	44.38±18.60	54.33±28.96	0.444
PLCO	64.00±17.72	64.85±18.71	0.928
PMCO	38.93±22.88	54.17±23.87	0.218
24 h after SAH			
CA1	14.65±14.68	31.12±34.33	0.333
CA2	24.67±15.42	48.03±33.87	0.175
CA2/3	49.72±7.13	61.73±26.35	0.345
CA3	42.69±20.19	44.68±23.52	0.876
DG	52.54±24.49	49.63±19.09	0.808
PLCO	59.60±11.83	75.08±23.63	0.2
PMCO	47.69±25.40	57.30±25.59	0.783
72 h after SAH			
CA1	21.10±19.74	30.07±20.90	0.486
CA2	29.69±29.65	32.54±17.71	0.847
CA2/3	45.74±28.54	52.36±25.01	0.691
CA3	30.32±19.24	50.24±26.51	0.196
DG	50.31±31.86	55.18±25.81	0.785
PLCO	66.43±12.46	77.59±13.05	0.183
PMCO	50.84±20.86	51.60±21.64	0.955

Note: Ar: Argon; CA: cornu ammonis; DG: dentate gyrus; PLCo: postero-lateral cortex; PMCo: postero-medial cortex; SAH: subarachnoid hemorrhage. Data are expressed as mean ± SD and analyzed by repeated measures analysis of variance.

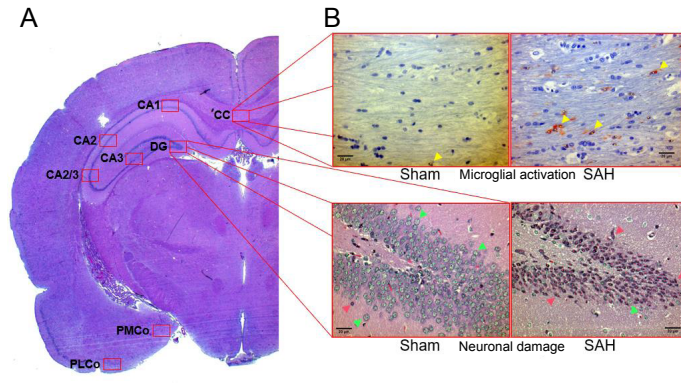


Figure 3: Effect of argon on the neuronal cell damage in the brain of SAH rats.

Note: (A) Selected regions of interest. A high-power field was focused on five regions of interest in the left hippocampus (CA1, CA2, CA2/3, CA3, DG) and two in the left cortex (PLCo and PMCo) and one in the corpus callosum (CC). (B) Upper: Microglial activation depicted by Iba-1 staining (exemplary section of corpus callosum; yellow arrows: Iba-1 positive microglia); Lower: Neuronal cell damage in hematoxylin-eosin staining exemplary for DG comparing SAH vs. sham surgery (green arrows: vital neurons; red arrows: dead neurons). CA: Cornu ammonis; DG: dentate gyrus; Iba-1: ionized calcium-binding adapter molecule 1; PLCo: postero-lateral cortex; PMCo: postero-medial cortex; SAH: subarachnoid hemorrhage.

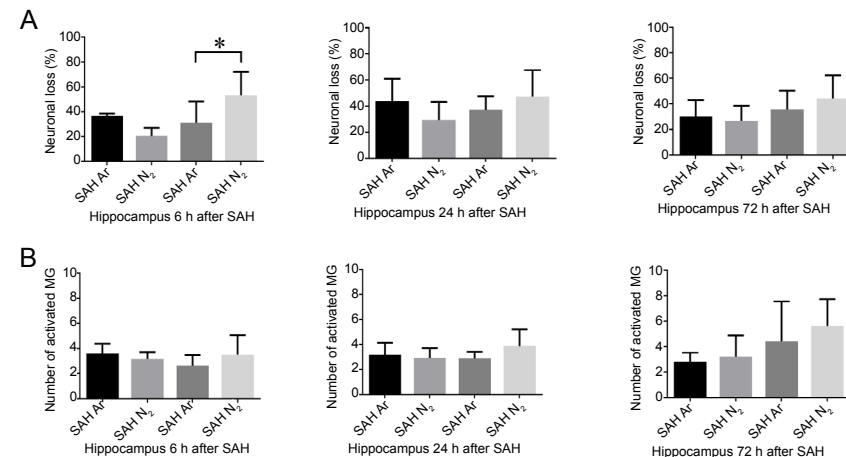


Figure 4: Hippocampal neuronal cell loss (A) and microglial activation (B) of the SAH rats with argon or N₂ treatment.

Note: Cytomorphological quantification of neuronal damage (A) and microglial activation (B) at 6, 24, and 72 hours after SAH. Microglial activation was expressed as number of activated microglia in 400-fold field. Data are expressed as mean ± SD. * $P < 0.05$ (repeated measures analysis of variance). Ar: Argon; MG: microglia; SAH: subarachnoid hemorrhage.

each ROI are displayed in **Table 2**. Hippocampal microglial activation did not differ between the treatment groups (6 hours after SAH: $P = 0.270$; 24 hours after SAH: $P = 0.192$; 72 hours after SAH: $P = 0.485$). At 24 hours after SAH the callosal microglia activation in the argon-treated group was significantly lower than in the control group (6 hours after SAH: $P = 0.064$; 24 hours after SAH: $P = 0.018$; 72 hours after SAH: $P = 0.436$; repeated-measures analysis of variance) (**Figure 6**), whereas 72 hours after SAH the difference was only seen for the cortical sum score (6 hours after SAH: $P = 0.574$; 24 hours after SAH: $P = 0.471$; 72 hours after SAH: $P = 0.034$; repeated-measures analysis of variance) (**Figure 5**). The sum scores are illustrated in **Figure 5**.

DISCUSSION

Our data indicate an effect of argon administration after experimental SAH on neuronal cell death and microglial activation pattern. Microglia plays a major role in the pro-inflammatory cytotoxic response and participates in the immunosuppressive processes contributing to further tissue damage.²¹ Reduction of microglial activation may attenuate secondary damage due to early brain injury. There is data from human specimen confirming this hypothesis: A causal link between microglia accumulation and neuronal cell death has been proposed.²² However, microglial activation may represent both devastating but also beneficial properties depending on its polarization.²³ Thus, microglia might play a biphasic action due to its polarization state. However, it has been argued that the concept of microglial polarization depicts a black and white pattern which does not properly reflect the physiologically smooth transition or even coexistence of both states.²⁴ It becomes even more complex if the multiple interactions of microglia with other cell types and possible communication via various pathways are taken into account.²⁵

Table 2: Microglial activation in the hippocampal CA1, CA2, CA2/3, DG, cortical PLCo, PMCo regions and CC of SAH rats

	SAH Ar	SAH N ₂	P-value
6 h after SAH			
CA1	2.11±0.75	3.28±1.85	0.184
CA2	2.39±0.61	2.78±1.53	0.576
CA2/3	2.67±1.76	3.17±2.08	0.663
CA3	2.78±1.97	3.17±2.09	0.748
DG	3.33±1.76	5.11±3.37	0.279
PLCO	5.72±1.00	5.44±0.34	0.532
PMCO	4.56±2.32	4.06±1.41	0.661
CC	2.56±0.83	4.06±1.56	0.064
24 h after SAH			
CA1	3.42±1.34	3.58±1.44	0.851
CA2	2.17±1.75	3.46±1.65	0.239
CA2/3	3.17±1.04	2.79±2.02	0.739
CA3	2.83±1.23	4.54±2.88	0.291
DG	2.92±1.42	5.04±2.62	0.166
PLCO	3.75±1.71	6.54±3.19	0.138
PMCO	4.42±2.08	3.71±2.83	0.669
CC	2.33 ± 0.47	6.04±2.55	0.018
72 h after SAH			
CA1	3.93±3.78	5.94±4.13	0.426
CA2	5.20±2.65	4.50±1.21	0.574
CA2/3	4.27±3.38	4.06±2.21	0.903
CA3	4.00±3.21	6.28±3.70	0.309
DG	4.60±4.42	7.39±4.45	0.326
PLCO	3.73±3.69	7.50±3.34	0.110
PMCO	3.00±2.54	6.50±2.07	0.033
CC	5.20±4.31	8.00±6.55	0.436

Note: Microglial activation was expressed as number of activated microglia in 400-fold field (mean ± SD). Ar: Argon; CA: cornu ammonis; CC: corpus callosum; DG: dentate gyrus; PLCo: postero-lateral cortex; PMCo: postero-medial cortex; SAH: subarachnoid hemorrhage. Data are expressed as mean ± SD and analyzed by repeated measures analysis of variance.

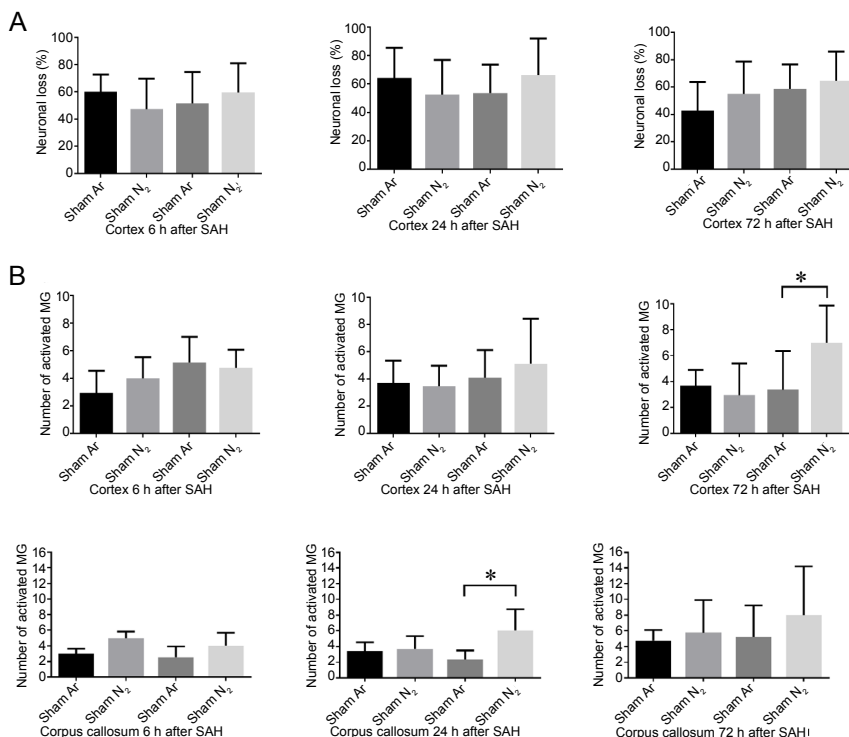


Figure 5: Cortical neuronal cell loss (A) and microglial activation (B) of the SAH rats with argon or N₂ treatment.

Note: Cytomorphological quantification of neuronal damage (A) and microglial activation (B) at 6, 24 and 72 hours after SAH. Microglial activation was expressed as number of activated microglia in 400-fold field. Data are expressed as mean ± SD. * $P < 0.05$ (repeated measures analysis of variance). Ar: Argon; MG: microglia; SAH: subarachnoid hemorrhage.

Figure 6: Microglial activation of the corpus callosum 6, 24 and 72 hours after SAH.

Note: Microglial activation was expressed as number of activated microglia in 400-fold field. Data are expressed as mean ± SD. * $P < 0.05$ (repeated measures analysis of variance). Ar: Argon; MG: microglia; SAH: subarachnoid hemorrhage.

We demonstrate a time-dependent activation pattern after experimental SAH (with increase of microglial activation over time), which is sporadically reduced in the argon treatment and affects also remote, white matter locations such as the corpus callosum. In contrast to our previously published data on xenon treatment after experimental SAH¹³ our currently published study is more heterogeneous and more difficult to interpret: At 24 and 72 hours after SAH there is a reproducible tendency of reduced microglial activation in the argon-treated group, which most probably due to low sample size and therefore underpowered experiments rarely reaches statistical significance. As previously described microglial activation increases over time. As previously depicted, the effect of argon treatment on secondary inflammation seems to peak at 24 hours after SAH.¹² However, there is no pronounced effect throughout the entire observation period. Whether the observed reduction of microglial activation represents a neuroprotective action of argon is not yet clear. Thus, especially concerning the specific localizations the data has to be confirmed examining a larger sample size.

Neuronal cell death after SAH as the primary outcome was significantly reduced in the hippocampal region 6 hours after SAH. This is in line with multiple studies demonstrating a neuroprotective effect by argon treatment (e.g., after experimental stroke, SAH but also after cardiac arrest).²⁶ However, we were not able to confirm the previously stated neuroprotective effects 24 hours after SAH, particularly those recently demonstrated for the dentate gyrus¹² as the protective effects seen here are rather located in other hippocampal areas but not the dentate gyrus. Further, the effect of reduced neuronal cell death diminishes with time, which may also represent a lack of sustainability of the argon treatment. The short treatment period (application of 50% argon for only 1 hour) also may account for the short-term effect. Thus, future strategies should evaluate a longer application of the noble gas. Altogether, our study does not generate a consistent proof of argon's neuroprotective and anti-inflammatory properties, which are most probably due to underpowered analyses (small sample sizes). However, there are also controversial data on argon's proposed neuroprotective action: Using a rodent model for cardiac arrest neither neurological nor histological improvement by argon could be shown recently.²⁷ Thus, larger (maybe multicentric) experimental studies and maybe in the future clinical trials have to be conducted to elucidate the potential of argon treatment.

Limitations

The relatively small number of cases in the individual groups, in particular in the sham groups (as low as $n = 2$), but also the treatment groups (not reaching estimated sample size) is a main limitation. Due to technical issues (e.g. insufficient quality of sections) animals had to be excluded resulting in a small sample size. Further, animals were treated within the framework of a controlled randomized study but analyses were performed thereafter. Thus, further inclusion of animals could not result in the mentioned small sample sizes.

Additionally, the sections were analyzed by one individual who was blinded for the treatment. A bias derived from subjective

interpretation is possible.

Further, no double staining to identify microglia has been performed. Iba-1 is a robust but not a specific marker for microglia. Further, no distinct NeuN staining to detect vital neurons has been carried out. Cell death has been quantified by morphological means.

Conclusion

The pattern of neuronal damage after experimental SAH seems to be modified by argon treatment resulting in an early decrease of neuronal damage, which unfortunately is not sustainable. Microglial activation in some regions (corpus callosum; basal cortex) is reduced in the argon-treated group 24 hours and 72 hours after SAH.

Author contributions

Animal experiments/immunohistochemistry, and data analysis: BK and AH; first draft of the manuscript: BK; support for histopathological examinations: KN, AW and MV; conception of study: MC and AH; assistance with data analysis and manuscript preparation: HC. All authors revised the manuscript and approved the final version.

Conflicts of interest

Parts of this manuscript have been presented at "70. Jahrestagung der Deutschen Gesellschaft für Neurochirurgie (DGNC)". AH lectured for Air Liquide. MC consulted and lectured for Baxter Healthcare and Air Liquide. His institution received grant support from the Deutsche Forschungsgemeinschaft (CO 799/9-1), Baxter Healthcare, and Air Liquide. All remaining authors have no potential conflict of interest to declare.

Financial support

This study was funded by the Start Program, RWTH Aachen. The funders had no role concerning study design, data collection and analysis, decision to publish, or preparation of the manuscript.

Institutional review board statement

The study protocol was approved by the Government Agency for Animal Use and Protection (Protocol number: TVA 10416G1; initially approved by "Landesamt für Natur, Umwelt und Verbraucherschutz NRW," Recklinghausen, Germany, on April 28, 2009).

Copyright license agreement

The Copyright License Agreement has been signed by all authors before publication.

Data sharing statement

The data could be shared if requested.

Plagiarism check

Checked twice by iThenticate.

Peer review

Externally peer reviewed.

Open access statement

This is an open access journal, and articles are distributed under the terms of the Creative Commons Attribution-NonCommercial-ShareAlike 4.0 License, which allows others to remix, tweak, and build upon the work non-commercially, as long as appropriate credit is given and the new creations are licensed under the identical terms.

REFERENCES

1. van Gijn J, Kerr RS, Rinkel GJ. Subarachnoid haemorrhage. *Lancet*. 2007;369:306-318.
2. de Rooij NK, Linn FH, van der Plas JA, Algra A, Rinkel GJ. Incidence of subarachnoid haemorrhage: a systematic review with emphasis on region, age, gender and time trends. *J Neurol Neurosurg Psychiatry*. 2007;78:1365-1372.
3. Wermer MJ, Greebe P, Algra A, Rinkel GJ. Long-term mortality and vascular event risk after aneurysmal subarachnoid haemorrhage. *J Neurol Neurosurg Psychiatry*. 2009;80:1399-1401.
4. Macdonald RL, Schweizer TA. Spontaneous subarachnoid haemorrhage. *Lancet*. 2017;389:655-666.



5. Fujii M, Yan J, Rolland WB, Soejima Y, Caner B, Zhang JH. Early brain injury, an evolving frontier in subarachnoid hemorrhage research. *Transl Stroke Res.* 2013;4:432-446.
6. Veldeman M, Höllig A, Clusmann H, Stevanovic A, Rossaint R, Coburn M. Delayed cerebral ischaemia prevention and treatment after aneurysmal subarachnoid haemorrhage: a systematic review. *Br J Anaesth.* 2016;117:17-40.
7. Höllig A, Schug A, Fahlenkamp AV, Rossaint R, Coburn M. Argon: systematic review on neuro- and organoprotective properties of an “inert” gas. *Int J Mol Sci.* 2014;15:18175-18196.
8. Ulbrich F, Goebel U. The Molecular Pathway of Argon-Mediated Neuroprotection. *Int J Mol Sci.* 2016;17:1816.
9. Loetscher PD, Rossaint J, Rossaint R, et al. Argon: neuroprotection in in vitro models of cerebral ischemia and traumatic brain injury. *Crit Care.* 2009;13:R206.
10. Liu J, Nolte K, Brook G, et al. Post-stroke treatment with argon attenuated brain injury, reduced brain inflammation and enhanced M2 microglia/macrophage polarization: a randomized controlled animal study. *Crit Care.* 2019;23:198.
11. Ryang YM, Fahlenkamp AV, Rossaint R, et al. Neuroprotective effects of argon in an in vivo model of transient middle cerebral artery occlusion in rats. *Crit Care Med.* 2011;39:1448-1453.
12. Höllig A, Weinandy A, Liu J, Clusmann H, Rossaint R, Coburn M. Beneficial properties of argon after experimental subarachnoid hemorrhage: early treatment reduces mortality and influences hippocampal protein expression. *Crit Care Med.* 2016;44:e520-529.
13. Veldeman M, Coburn M, Rossaint R, et al. Xenon reduces neuronal hippocampal damage and alters the pattern of microglial activation after experimental subarachnoid hemorrhage: a randomized controlled animal trial. *Front Neurol.* 2017;8:511.
14. Kilkenny C, Browne WJ, Cuthill IC, Emerson M, Altman DG. Improving bioscience research reporting: the ARRIVE guidelines for reporting animal research. *PLoS Biol.* 2010;8:e1000412.
15. Höllig A, Weinandy A, Nolte K, Clusmann H, Rossaint R, Coburn M. Experimental subarachnoid hemorrhage in rats: comparison of two endovascular perforation techniques with respect to success rate, confounding pathologies and early hippocampal tissue lesion pattern. *PLoS One.* 2015;10:e0123398.
16. Park IS, Meno JR, Witt CE, et al. Subarachnoid hemorrhage model in the rat: modification of the endovascular filament model. *J Neurosci Methods.* 2008;172:195-200.
17. Hockel K, Trabold R, Schöller K, Török E, Plesnila N. Impact of anesthesia on pathophysiology and mortality following subarachnoid hemorrhage in rats. *Exp Transl Stroke Med.* 2012;4:5.
18. Paxinos G, Watson C. *The Rat Brain in Stereotaxic Coordinates.* 7th ed. Amsterdam: Academic Press. 2013.
19. Imai Y, Ibata I, Ito D, Ohsawa K, Kohsaka S. A novel gene iba1 in the major histocompatibility complex class III region encoding an EF hand protein expressed in a monocytic lineage. *Biochem Biophys Res Commun.* 1996;224:855-862.
20. Vinet J, Weering HR, Heinrich A, et al. Neuroprotective function for ramified microglia in hippocampal excitotoxicity. *J Neuroinflammation.* 2012;9:27.
21. Perego C, Fumagalli S, De Simoni MG. Temporal pattern of expression and colocalization of microglia/macrophage phenotype markers following brain ischemic injury in mice. *J Neuroinflammation.* 2011;8:174.
22. Schneider UC, Davids AM, Brandenburg S, et al. Microglia inflict delayed brain injury after subarachnoid hemorrhage. *Acta Neuropathol.* 2015;130:215-231.
23. Ma Y, Wang J, Wang Y, Yang GY. The biphasic function of microglia in ischemic stroke. *Prog Neurobiol.* 2017;157:247-272.
24. Ransohoff RM. A polarizing question: do M1 and M2 microglia exist? *Nat Neurosci.* 2016;19:987-991.
25. Kettenmann H, Hanisch UK, Noda M, Verkhratsky A. Physiology of microglia. *Physiol Rev.* 2011;91:461-553.
26. Brücken A, Kurnaz P, Bleilevens C, et al. Dose dependent neuroprotection of the noble gas argon after cardiac arrest in rats is not mediated by K(ATP)-channel opening. *Resuscitation.* 2014;85:826-832.
27. Zuercher P, Springe D, Grandgirard D, et al. A randomized trial of the effects of the noble gases helium and argon on neuroprotection in a rodent cardiac arrest model. *BMC Neurol.* 2016;16:43.

Received: November 21, 2019

Accepted: February 15, 2020

Published Online: September 30, 2020